Deuterium effusion from nanocrystalline boron nitride thin films

2001 J. Phys.: Condens. Matter 13 5853

(http://iopscience.iop.org/0953-8984/13/26/301)

INSTITUTE OF PHYSICS PUBLISHING JOURNAL OF PHYSICS: CONDENSED MATTER

J. Phys.: Condens. Matter **13** (2001) 5853–5864 www.iop.org/Journals/cm PII: S0953-8984(01)21812-8

Deuterium effusion from nanocrystalline boron nitride thin films

R Checchetto[1], **A Miotello and R S Brusa**

Istituto Nazionale per la Fisica della Materia (INFM) and Dipartimento di Fisica dell'Università di Trento, I-38050 Povo (TN), Italy

E-mail: checchet@science.unitn.it

Received 9 February 2001, in final form 12 April 2001

Abstract

Deuterium thermal desorption experiments were performed on hexagonal (h-BN) and cubic (c-BN) boron nitride thin films deposited on (100) oriented Si substrate by radio frequency (rf) magnetron sputtering. BN samples were deuterated by thermal annealing at 673 K in a 10^{-4} mbar D_2 atmosphere for 100 min. No differences were observed between c-BN and h-BN thin film samples in the effusion process, which occurred through a thermal activated heterogeneous first order kinetics. The activation energy for desorption exhibited a Gaussian distribution peaked at 2.28 ± 0.01 eV with 0.18 ± 0.02 eV semidispersion. This result indicated the breaking of the N–D and B–D chemical bonds, probably located at the grain boundaries of the nanocrystalline material, as the rate limiting step in the effusion kinetics. When the deuteration of the BN thin film samples occurred by 20 keV D_2 ion implantation, deuterium effusion is controlled by the migration of deuterium atoms to the sample surface through grain boundaries path and is characterized by 0.52 ± 0.03 eV activation energy.

1. Introduction

Boron nitride is a III–V compound material which can crystallize with a hexagonal (h-BN) and a cubic (c-BN) structure. Hexagonal boron nitride is chemically inert, thermally stable and has a direct electronic band gap close to 4 eV: recently it was proposed as boron diffusion source and gate insulator for a metal–insulator–semiconductor field effect transistor (MISFET) [1]. Cubic boron nitride (c-BN) has very high hardness (4500–5500 HV), high melting point (3300 K), good thermal conductivity (13 W cm^{-1} K^{-1}) and presents an indirect band gap value of 6.0–6.4 eV, which is the largest of all elemental and III–V compounds. Being dopable both as a p type (with Be, for example) and an n type (with Si, for example) semiconductor [2], there is a growing interest for this material in special applications such as, for example, high temperature semiconductor devices [3].

[1] Corresponding author.

0953-8984/01/265853+12$30.00

The bonding of hydrogen in hexagonal (h-BN) and cubic (c-BN) boron nitride was recently theoretically investigated by Widany *et al* [4] using a density-functional method based on an orthogonal tight-binding scheme. The most important conclusion drawn by the authors was the very different behaviour of hydrogen atoms in the two BN phases. Hydrogen atoms can have three stable configurations in c-BN: the bonded nitrogen related C-position (C_N), the bond centred configuration (BC) and the non-bonded tetrahedral position (T_B) but all of them are energetically unfavoured relative to free hydrogen. In contrast, in h-BN, the two stable configurations also turn out to be energetically favoured: the non-bonding and the bonding interlayer sites result, in fact, in energy gain, relative to free hydrogen, of -0.98 and -0.92 eV, respectively. This theoretical result indicates that in c-BN films, hydrogen atoms should be mostly found in the hexagonal part of the film (a hexagonal component in an already formed c-BN film is almost always present) or in the boundaries of the grains in cubic phase: this indication is supported by some experimental investigations [5, 6]. Kuhr *et al* [5] studied by elastic recoil detection analysis (ERDA) the hydrogen content in CVD deposited c-BN films and observed that in the sp^2 bonded nucleation layer the hydrogen content was close to 25 at.% while in the rest of the films, that is the layers grown with cubic structure, the H concentration was lower than 15 at.%. Recently we studied the deuterium content in h-BN and c-BN thin films previously subjected to deuterium permeation experiments [6]. The deuterium concentration profiles, obtained by ERDA measurements, indicated that: (a) the deuterium content in the h-BN film was quite higher than the deuterium content in the c-BN one, (b) in the h-BN film deuterium was uniformly distributed along the film thickness but in the c-BN sample deuterium atoms were mainly located in the sp^2 bonded nucleation layers.

In this paper we present an experimental study on the effusion of deuterium from hexagonal (h-BN) and cubic (c-BN) boron nitride thin films based on thermal desorption spectroscopy (TDS) analysis. Deuterium was inserted in the BN layers by two different procedures: (a) low temperature thermal annealing in a 10^{-4} mbar D_2 atmosphere, or (b) 20 keV D_2 ion implantation.

The two procedures give rise to different release mechanisms of the deuterium atoms contained in the BN film. Low temperature thermal annealing introduces, in fact, deuterium close to the surface BN layers without producing any crystalline damage. By ion implantation, in contrast, deuterium is driven far from the sample surface and crystalline damage, mainly point defects and small defect clusters, is produced in the ion implanted atomic layers. A simple model to analyse the effusion of deuterium from a solid matrix considers the kinetics as governed by the competition between three elementary processes: (a) the release of deuterium atoms from the sites where they are contained in the host BN lattice, (b) the deuterium atomic diffusion to the sample surface and (c) the recombinative desorption of deuterium atoms from the surface to the gas phase. While the sample prepared by low temperature thermal annealing offers the possibility of studying the role of processes (a) and (c), in the ion implanted samples, deuterium atoms being located far from the BN surface, the role of the diffusion process in the effusion kinetics can be also appreciated.

2. Experiment

Nearly stoichiometric BN thin films 500 nm thick, were deposited on chemically cleaned (100) oriented Si wafers by rf magnetron sputtering using sintered h-BN with nominal purity of 97.5 at.% as target material and a mixture of 97 at.% Ar and 3 at.% N_2 as working gas. At 150 W rf target power nanocrystalline BN thin films crystallized with hexagonal or cubic structure were obtained with -50 and -100 V substrate bias voltage, respectively. The structure of the rf sputter deposited BN sample was studied in a previous paper [7]. The deposited samples turn

out to be nearly stoichiometric showing a B/N atomic compositional ratio = 1.1, as observed by Auger electron spectroscopy (AES). By glancing angle x-ray diffraction analysis (XRD) we observed that the deposited h-BN film grows with the (002) planes oriented normal to the substrate, while the c-BN layers turn out to be (111) oriented. By the Scherrer analysis of the XRD diffraction peak we deduced a correlation length of 1.6 and 1.5 nm for h-BN and c-BN thin films respectively, indicating grain size in the nanocrystalline range.

Deuterium was absorbed by the samples through thermal annealing in a 10^{-4} mbar D_2 atmosphere: the process was carried out at 673 K for 100 min in a stainless steel chamber with base pressure in the low 10^{-7} mbar range. To avoid deuterium losses, the samples were rapidly cooled in the annealing chamber by flowing high purity Ar gas over their surface. Deuterium was inserted in the samples also by room temperature D_2 ion implantation at 20 keV D_2^+ energy and 3×10^{16} D_2^+ cm^{-2} fluence. Simulations performed by the TRIM code [8] indicate that all the implanted deuterium ions are contained in the BN layers: the medium projected range, R_P, of the ions is 155 nm while their longitudinal straggling, ΔR_P, is 35 nm.

The crystalline phase of the BN thin films deposited with different substrate bias voltages and the deuterium chemical bonding were examined by Fourier transform infrared spectroscopy (FTIR): spectra were taken at room temperature in dry air in the 500–3000 cm^{-1} spectral range with 4 cm^{-1} resolution.

Thermal desorption spectroscopy (TDS) analyses were performed in an UHV stainless steel chamber pumped by a turbomolecular pump and equipped with a quadrupole mass spectrometer (QMS) [9]. The experiments were carried out by heating the sample with a linear temperature ramp of 0.5 K s^{-1} up to ∼1100 K (which is the temperature limit of our sample holder) and measuring the QMS D_2^+ mass signal ($m/e = 4$). At constant pumping speed of the vacuum apparatus the QMS signal is directly proportional to the value of the deuterium effusion rate. The absolute value of the D_2 effusion flux from our BN thin films was obtained by comparing the effusion signal with that measured, in the same experimental conditions, by using a reference D implanted Al thin film. Experimental errors in the deuterium effusion signal were estimated from the mean value of the fluctuations in the $m/e = 4$ background level.

The open volume defect distribution in the as deposited and ion implanted h-BN thin films was studied by positron annihilation spectroscopy (PAS). The Doppler broadening of the 511 keV annihilation line, due to the electron–positron momenta, was measured using a slow positron beam coupled with a high purity Ge detector with a resolution of 1.2 keV at 511 keV. The shape of the annihilation line was characterized by the S parameter, i.e. the fraction of positrons annihilating with electrons in the low momentum range ($p_l = 0$–$0.33 \times 10^{-3}\ m_0 c$, where p_l is the electron–positron momentum component in the detector direction). In a defected material, positrons are efficiently trapped into open volume defects. This trapping produce an increase of positron annihilation rate with electrons of low momenta signalled by the increase of the S parameter [10]. The S parameter was measured as a function of the mean positron implantation depth $x = (40/\rho)E^{1.6}$ nm (where $\rho = 2.25$ g cm^{-3} is the density of our films, and E the positron energy in keV) in the 0.2 nm–2 μm range.

3. Results

In figure 1 we present the measured deuterium effusion rate (solid points) as a function of the sample temperature for the BN thin films deuterated by thermal annealing in D_2 atmosphere. We observed very similar effusion kinetics in both the samples crystallized in cubic and hexagonal phases: the effusion kinetics in c-BN film and h-BN thin films, see figures 1(a) and 1(b) respectively, is characterized by very broad effusion peaks (FWHM ∼ 200 K) with

peak temperature T_P at ∼700 K. The only relevant difference between hexagonal and cubic samples is a tail on the high temperature side exhibited by the h-BN thin film.

In figure 2(a) we present the measured deuterium effusion flux (solid symbols) as a function of the sample temperature for the D_2 ion implanted h-BN thin films. The D_2 release from the ion implanted h-BN sample occurs at temperatures higher than that observed for the samples deuterated in D_2 atmosphere and is characterized by a very broad effusion peak: the steep decrease of the effusion signal occurring at $T \sim 1100$ K is an experimental artefact related to the upper limit of the temperature ramp. In figure 2(b) we present the measured effusion flux (solid symbols) as a function of the sample temperature for the D_2 ion implanted c-BN thin film. Comparing this spectrum with the spectrum pertinent to the ion implanted h-BN thin film, we observe that the D_2 effusion occurs at lower temperatures and is characterized by narrow effusion peaks between 400 and 600 K.

In figure 3 we show the S parameter curves as function of the mean positron implantation depth for the D_2 ion implanted h-BN thin films: curve (a) is pertinent to the as-deposited sample, curve (b) to the sample after deuterium ion implantation and curve (c) to the implanted sample after thermal annealing at 900 K. The S values in the curves are normalized with respect to the substrate bulk Si value (S_{Si}). The increase of the S parameter in the film thickness (curves (b) and (c)) with respect to curve (a) denotes an increase of open volume defects after D_2 ion implantation also after thermal annealing of the implanted sample.

4. Discussion

4.1. Deuterium effusion from BN thin films annealed in D_2 atmosphere

When the effusion kinetics can be described as a process characterized by a single thermal activated process having a defined activation energy E, the effusion rate $r(t)$ is given by [11]

$$r(t) = -\frac{\mathrm{d}C}{\mathrm{d}t} = -\frac{C^n}{\tau(T, E)} \tag{1}$$

where $\tau(T, E) = \tau_0 \exp(E/k_B T)$ is a characteristic time, a function of the sample temperature T (in our experiment $T = T_0 + \alpha t$, α is the temperature ramp); n is the order of the reaction. If C_0 is the total amount of deuterium involved in the effusion process then the solution of equation (1) with initial condition $C(0) = C_0$, is given by

$$C(t) = C_0 \exp\left(-\frac{t}{\tau(T, E)}\right) \tag{2}$$

and the effusion rate $r(t)$ can be calculated as

$$r(t) = -\frac{\mathrm{d}C}{\mathrm{d}t} = \frac{C_0}{\tau} \exp\left(-\frac{t}{\tau}\right). \tag{3}$$

The best fit of the experimental effusion peak was obtained by using $\tau_0 = 10^{-13}$ s^{-1} and $E = 2.28$ eV (see the simulation reported in figure 1(a) as a dotted line). As clearly evident the adopted model (equation (1)) cannot explain the present experimental data because we only reproduce the peak position at ∼700 K but the experimental desorption peak has a much broader width ($\Delta T \sim 200$ K) than the simulated one ($\Delta T \sim 100$ K).

To reproduce the experimental data we have to consider the effusion process as characterized by heterogeneity in the thermal activated process [11]. We can consider this heterogeneity by introducing a distribution function $\varphi(E)$ for the activation energy, where $\varphi(E)\,\mathrm{d}E$ represents the fraction of deuterium that desorbs with activation energy values between E and $E + \mathrm{d}E$. The normalization condition requires that $\int_0^\infty \varphi(E)\,\mathrm{d}E = 1$.

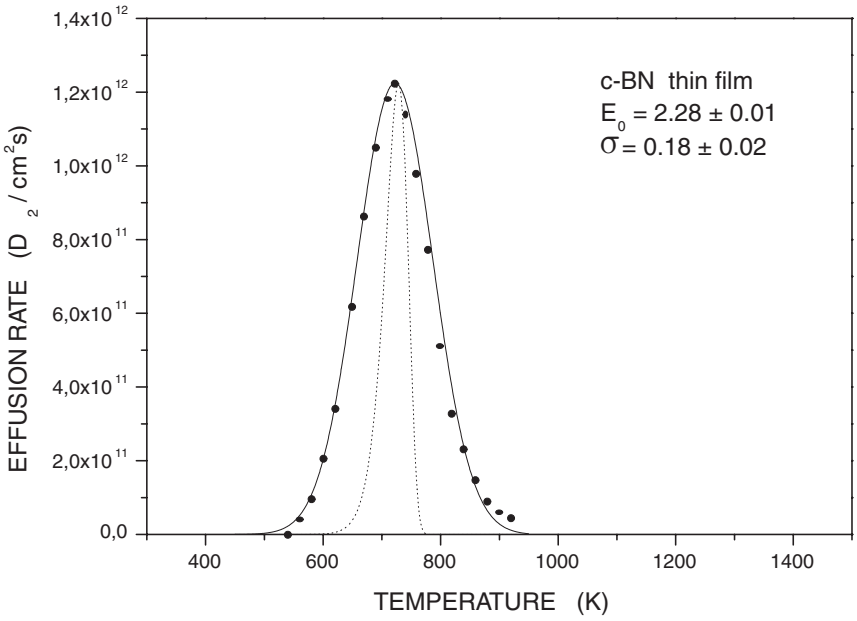

(a)

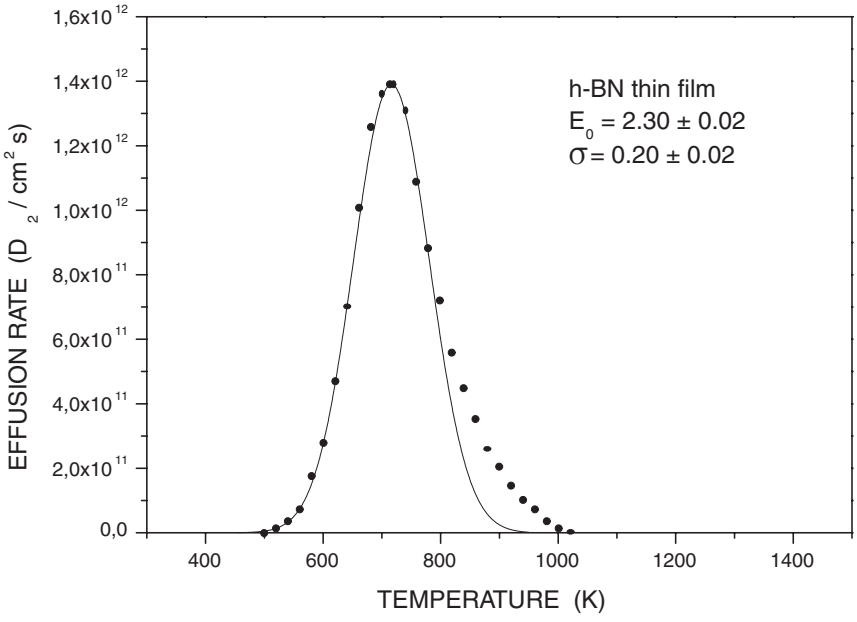

(b)

Figure 1. (a) TDS spectrum of c-BN thin film annealed in D_2 atmosphere. Experimental data are reported as solid symbols. The solid line is a numerical simulation of the data pertinent to a heterogeneous first order process. The dotted line is a simulation pertinent to a homogeneous first order process. (b) TDS spectrum of h-BN thin film annealed in D_2 atmosphere. Experimental data are reported as solid symbols. The solid line is a numerical simulation of the data pertinent to a heterogeneous first order process.

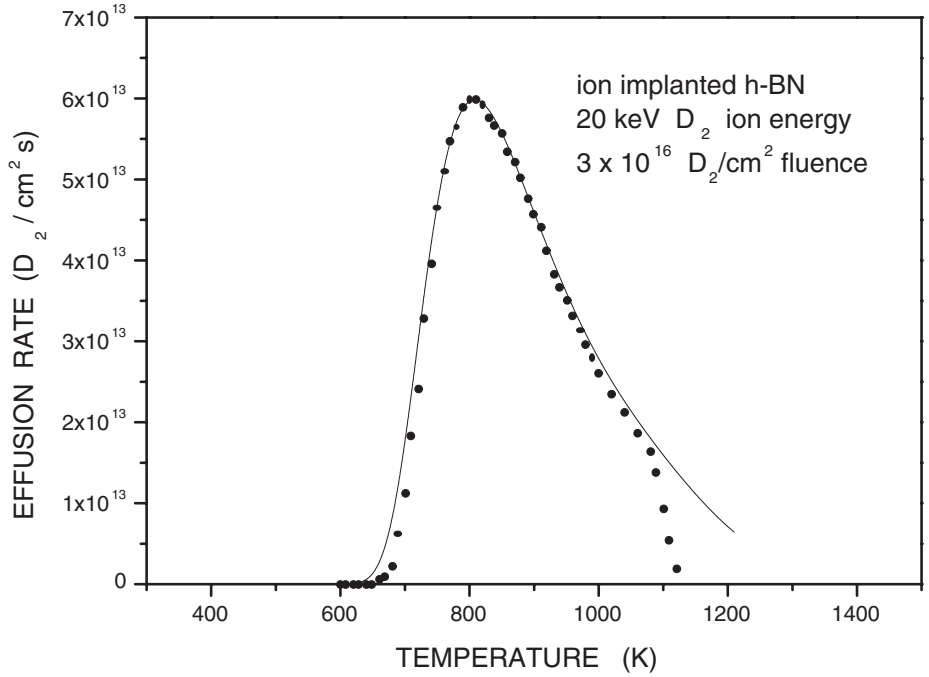

(a)

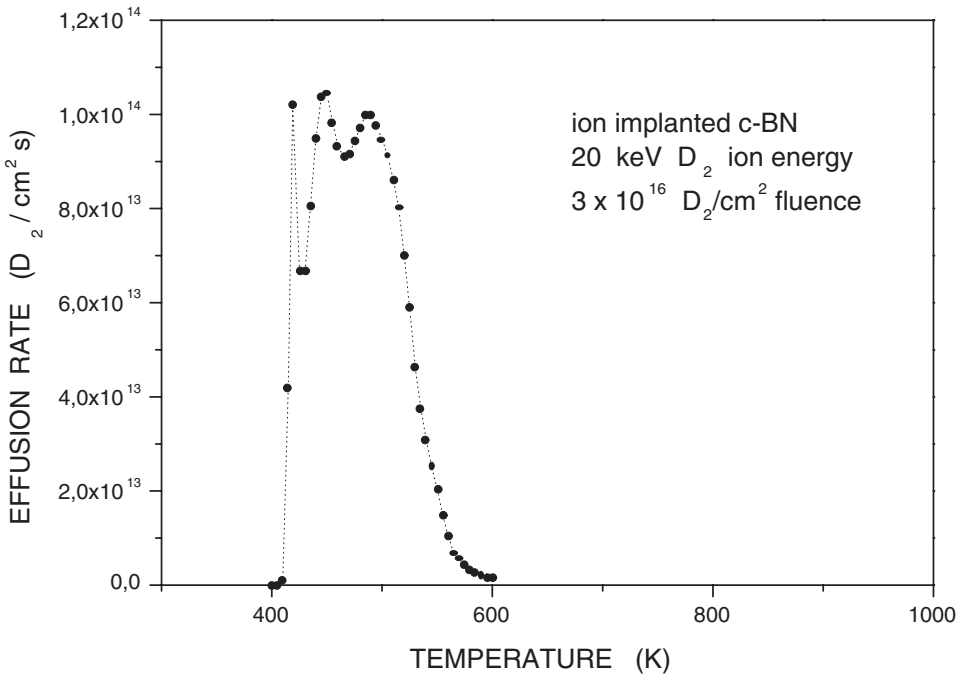

(b)

Figure 2. (a) TDS spectrum of D_2 ion implanted h-BN thin film. Experimental data are reported as solid symbols. The solid line is the numerical simulation of the data pertinent to a diffusion limited effusion process. (b) TDS spectrum of D_2 ion implanted c-BN thin film. Experimental data are reported as solid symbols; the dotted line is just a guide for the eye.

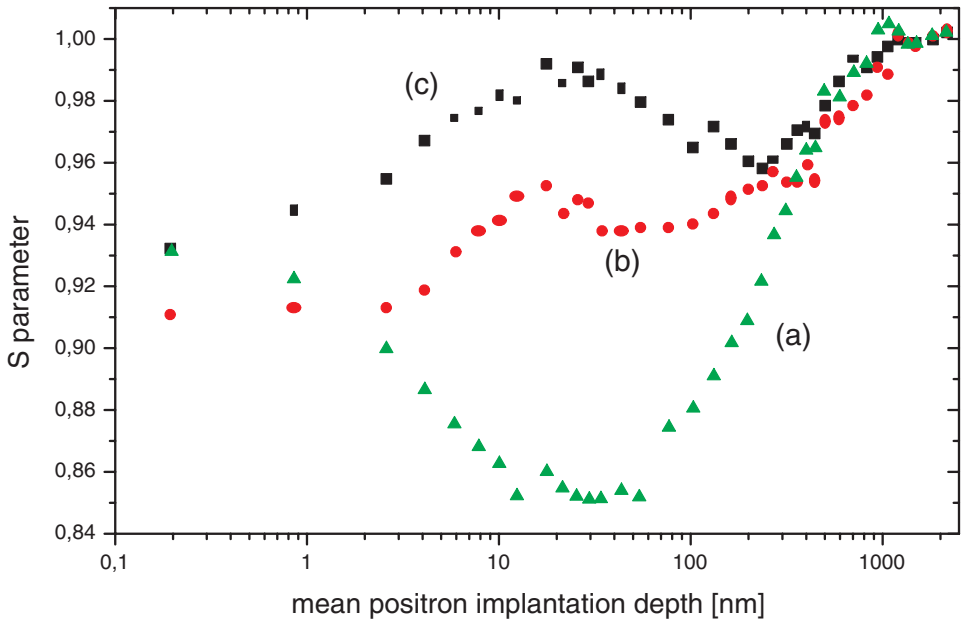

Figure 3. *S* parameter of the Doppler broadening annihilation line against positron implantation energy for the h-BN thin film: full triangles (curve (a)) are pertinent to the as-deposited sample, full circles (curve (b)) to the D_2 ion implanted sample and full squares (curve (c)) to the D_2 ion implanted sample after UHV thermal annealing at 900 K.

The solution of equation (1) can be obtained by weighting the contribution of each site characterized by the activation energy E to the effusion flux $r(t)$ by its own probability

$$C_h(t) = \int_0^\infty C(t, E)\varphi(E)\,\mathrm{d}E. \tag{4}$$

According to equation (2) we used the family of functions

$$C(t, E) = C_0 \exp\left(-\frac{t}{\tau_0 \exp(E/k_B T)}\right) \tag{5}$$

as a kernel of equation (4) and the effusion rate was calculated by assuming for the activation energy a Gaussian distribution

$$\varphi_{E_0,\sigma}(E) = \frac{1}{\sigma\sqrt{2\pi}} \exp\left(-\frac{(E - E_0)^2}{2\sigma^2}\right). \tag{6}$$

In figures 1(a) and 1(b) we report, as a solid line, the simulation of the effusion data calculated by assuming for both c-BN and h-BN samples a first order kinetics ($n = 1$). The D_2 effusion data pertinent to the c-BN sample were fitted with $E_0 = 2.28 \pm 0.01$ eV and $\sigma = 0.18 \pm 0.02$ eV, while data pertinent to the h-BN sample were reproduced with $E_0 = 2.30 \pm 0.02$ eV and $\sigma = 0.20 \pm 0.02$ eV.

Such a high value of the desorption energy strongly suggests the breaking of deuterium related chemical bonds as the rate limiting process in the effusion kinetics from h-BN and c-BN thin films. Deuterium being released as a molecule, the values of the activation energy for desorption, E_{des}, can be related to the strength E_{BN-D} of the chemical bond through the equation $2E_{BN-D} = E_{des} + E_{D-D}$ [12], where E_{D-D} is the binding energy of the D_2 molecule

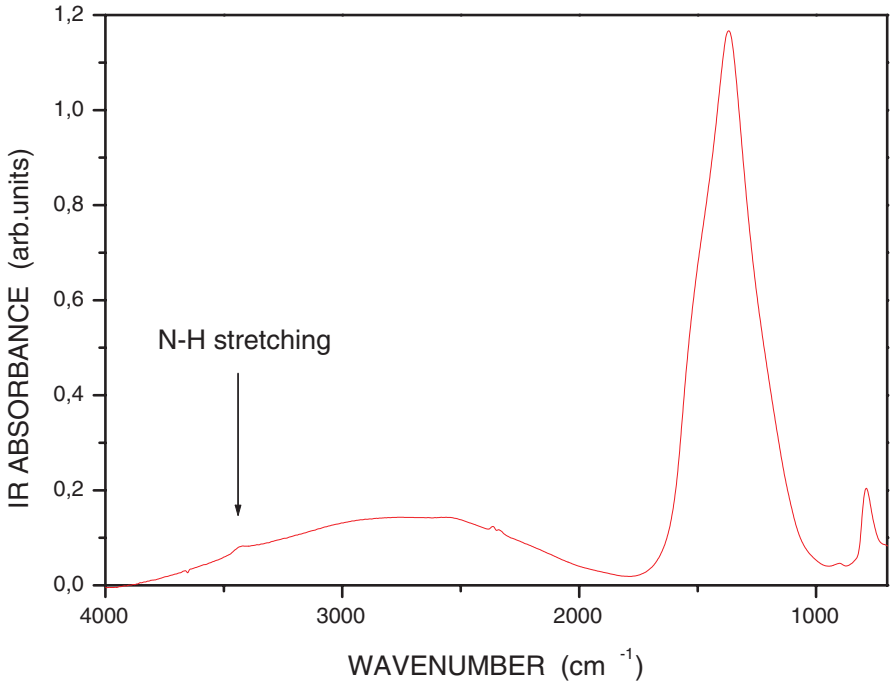

Figure 4. FTIR spectrum of the as deposited h-BN thin film on Si substrate.

(this approach assumes as negligible the energy barrier for adsorption). Considering that the binding energy of the deuterium molecule is 4.45 eV [13], the value of 2.28 eV for E_{des} indicates that the binding energy of a deuterium atom with the BN host is 3.36 ± 0.02 eV. This value is very close to the value of 3.25 ± 0.18 eV pertinent to the nitrogen–hydrogen (N–H) bond strength [13] and to the value of 3.49 ± 0.56 eV pertinent to the boron–hydrogen bond strength [13] and indicates chemical deuterium bonding with the host atomic network. The heterogeneity in the activation energy can be explained by considering that B–D and N–D chemical bonding likely occurs in the grain boundary of the nanostructured BN thin films where the less ordered BN structure gives rise to different bonding configurations.

It is important to remark that the similar behaviour in the deuterium effusion kinetics presented by h-BN and c-BN thin films is related to the defects present in the two host BN systems. Both samples present a high fraction of grain boundaries volume and deviation from stoichiometry, the deposited films being rich in boron.

To conclude this part of the discussion it is interesting to compare the physical–chemical state of the absorbed deuterium atoms with that of the hydrogen atoms contained as atomic impurity in the as deposited layers. Owing to the presence of H_2O vapour in the residual vacuum of the deposition chamber, sputter deposited films contain H atoms whose concentration is typically in the 1 at.% range [14] and uniformly distributed through the film thickness. In figure 4 we present the FTIR analysis of the as deposited h-BN sample: in the spectrum we only observe a weak IR absorption peak at $\sim$3450 cm^{-1} pertinent to the N–H stretching vibration [15] indicating that at least a part of the this hydrogen is chemically bonded, that is the same condition as absorbed D atoms: after thermal annealing at 800 K temperature this signal disappears.

4.2. Deuterium effusion from ion implanted BN thin films

In metallic thin films the hydrogen migration to the sample surface is a very fast process and, as a consequence, hydrogen effusion results controlled by release of atomic hydrogen from interstitial or trapping sites in the host lattice [16] or by surface recombination [17]. This is not generally true in ceramic and semiconductor materials where effusion can be controlled by diffusion through the host atomic network owing to the defect structure of the material [18, 19]. An important indication which can be obtained by observing the release kinetics from the ion implanted h-BN sample is that deuterium desorption occurs at temperatures higher than the typical temperatures of deuterium effusion from annealed samples. This clearly indicates that the release kinetics is governed by processes which are different from the release of deuterium from chemically bonded states. In the present BN samples implanted deuterium is distributed in atomic layers far (∼160 nm) from the sample surface and a simple estimate indicates that the diffusion process can be effective. Published data on deuterium diffusivity in h-BN [20] show that τ_{diff}, that is the interval time involved in the diffusion from the ion implanted region to the h-BN surface, is of the same order as τ_{des}, the characteristic time for deuterium desorption. We can, in fact, estimate τ_{diff} by the random-walk expression $\tau_{diff} = R_P^2/D$ (at 600 K, when effusion starts, the deuterium diffusion constant is of the order of 10^{-12} cm^2 s^{-1} [18]) and τ_{des} by the relation T_P/α ($T_P \sim 800$ K is the temperature peak in the effusion rate and $\alpha = 0.5$ K s^{-1} the temperature ramp).

We thus studied the deuterium effusion from the ion implanted h-BN thin film by considering diffusion as the rate limiting process thus solving the one dimensional diffusion equation [21]:

$$\frac{\partial c}{\partial t} = D\frac{\partial^2 c}{\partial x^2} \tag{7}$$

where $c = c(x, t)$ is the deuterium concentration at depth x and time t and D the diffusion coefficient of deuterium atoms. The diffusion equation was solved with a Gaussian form for the initial deuterium concentration profile:

$$c(x, t = 0) = A\exp[(x - x_0)^2/\Delta x_0^2] \tag{8}$$

assuming for x_0 and Δx_0 the values of medium projected range R_P and straggling ΔR_P of the implanted deuterium ions as calculated with the TRIM code. The deuterium effusion flux was calculated as

$$J_{eff} = -D\left.\frac{\partial c}{\partial t}\right|_{x=0}. \tag{9}$$

The solid line in figure 2(a) is a numerical fit of the experimental data based on the previous model. We assumed that the diffusion process was described by an activated diffusion coefficient $D(T) = D_0\exp(-E_D/k_BT)$ and the best fit was obtained with $E_D = 0.53 \pm 0.03$ eV and $D_0 \sim 10^{-9}$ cm^2 s^{-1}. The values obtained for both activation energy E_D and pre-exponential factor D_0 are in excellent agreement with the values 0.52 ± 0.04 eV and $\sim 10^{-8}$ cm^2 s^{-1}, respectively, obtained by studying with the permeation technique the deuterium diffusion process through h-BN thin films [20] grown by rf sputtering with the same deposition parameters. We indicated [20] that the deuterium migration process was controlled by the diffusion of deuterium atoms in the volume fraction of the h-BN film through grain boundaries, as suggested by the structure of the deposited layers, which consists of nanocrystals with 2–3 nm average diameter. Here we also suggest that grain boundary diffusion is the rate limiting process in the deuterium effusion from the ion implanted h-BN samples.

Some more information on the sites where the ion implanted deuterium is accommodated can be obtained by the analysis of the positron annihilation spectra presented in figure 3. In the

as-deposited h-BN film, the S parameter starts from a certain surface value, decreases to the S value ($\sim$0.85) characteristic of our h-BN film and then increases monotonically through the interface reaching the S_{Si} value. This monotonic increase from the S value of the film to the S_{Si} value indicates that there are no positron trapping centres at the interface. The spectrum pertinent to the ion implanted sample is quite different: the S parameter is, at any depth of the h-BN film, higher than in the as-deposited film clearly indicating the presence of open volume defects consequent to the damage created by the deuterium implantation process. Thermal annealing at 900 K produces a further increase of the S parameter revealing the appearance of more open volume defects. At this temperature, as we deduced from figure 2, more than 80% of the implanted deuterium atoms were released from our sample and the increase of the open volume defects indicates that deuterium occupied a part of them (which were consequently seen by positrons as passivated traps [22, 23]). Like hydrogen [24], deuterium is expected to decorate the open volume defects forming B–D and N–D bonds or to fill them as D_2 molecules. To make inferences about the chemical–physical state of implanted deuterium in h-BN samples we performed accurate Fourier transform infra-red analysis (FTIR): before going on with the IR results we remark that in bulk silicon implanted hydrogen turns out to be chemically bonded to silicon and that IR signals pertinent to many kinds of hydrogen-related centres have been clearly detected by FTIR also for implantation fluence as low as 2×10^{16} H_2^+ cm^{-2} [24]. We thus expected to find IR signals on the present 3×10^{16} D_2^+ cm^{-2} implanted h-BN samples. It is known that B–H and N–H stretching vibrations produce IR absorption peaks at 2525 cm^{-1} and 3450 cm^{-1} [15] and we expected to find deuterium related signals at $\sim$1785 and $\sim$2440 cm^{-1}: these signals have not been observed. Although this is quite surprising taking into account the extraordinary chemical reactivity of hydrogen isotopes with defects in semiconductor material, we conclude that in the open volume defects the implanted deuterium does not form chemical bonds but is contained as D_2 molecules. In sputter deposited nanocrystalline silicon films Lusson *et al* [25] observed by transmission electron microscope analysis (TEM) the presence of microcavities large enough to trap deuterium in molecular form. The authors observed that, deuterium atoms being the only diffusing species, the rate limiting step in the deuterium effusion was the D_2 molecular dissociation in the internal surface of these microcavities, which was effective in their nanocrystalline Si sample at temperatures higher than 650 °C. Having this in mind, let us consider our h-BN samples; if implanted deuterium is contained as a molecule in extended voids, then the experimental result of Lusson *et al* [25] clearly indicates that at the observed effusion temperatures, see figure 2(a), the D_2 molecular dissociation at the internal surface of the voids has to occur. We have not found in the literature any experimental result on the D_2 kinetics on BN surfaces and thus, to check this point, we performed D_2 permeation measurements through an h-BN coated stainless steel membrane (in the form of a thin disc) in the 473–763 K temperature range. In these experiments the coated side of the sample was exposed to D_2 gas while the uncoated side to an UHV chamber where the vacuum conditions were controlled by mass spectrometer. The permeation process being the combined effect of (a) the D_2 molecular dissociation at the h-BN surface exposed to the gas, (b) the D atomic absorption, (c) diffusion in the h-BN bulk and (d) the recombinative desorption process [26], then the detection of a permeation signal at a certain temperature indicates that all the processes (a)–(d) are efficient at such temperature. In figure 5 we present the permeation fluxes measured at two different temperatures: the strong increase of the permeation flux when passing from 613 to 673 K suggests that all processes (a)–(d) are really efficient.

The process of deuterium effusion from ion implanted h-BN thin films can thus be described in this way: after ion implantation, implanted deuterium is contained as D_2 molecules in the extended voids present in the h-BN layers. During the TDS run these molecules are first dissociated at the internal h-BN surfaces of these microcavities and then D atoms diffuse

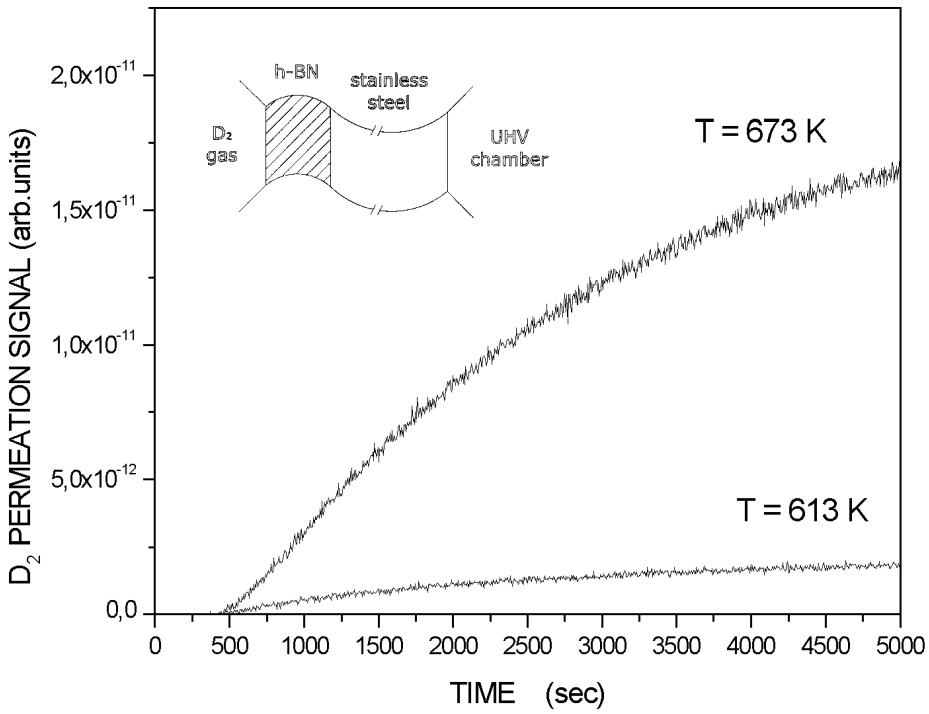

Figure 5. Deuterium permeation flux through h-BN thin films deposited on stainless steel substrate. In the figure we indicate the experimental geometry.

to the sample surface where desorption occurs. We describe our experimental data on the deuterium effusion by considering the diffusion process, thus proving that in this system the atomic diffusion is the rate limiting step.

We conclude this part by discussing the results of the experiments carried out on D_2 ion implanted c-BN samples. The very different effusion kinetics is on our opinion not an effect related to the different crystalline structure because deuterium thermal effusion is controlled by grain boundary diffusion and both hexagonal and cubic crystallized samples have the same nanocrystalline structure with nearly equal grain size. The different effusion curves are simply related to the sample conditions after ion implantation. c-BN samples, in fact, appeared immediately delaminated and presented macroscopic defects such as cracks which are detectable also by the naked eye.

5. Conclusions

We have studied the deuterium effusion from boron nitride thin films deposited by rf magnetron sputtering. When deuteration of the samples is carried out by 673 K thermal annealing in a low pressure D_2 atmosphere, deuterium effusion occurs through a first order kinetics for both c-BN and h-BN thin films and shows heterogeneity in the activated process governing effusion: the energy values turn out to be peaked at about 2.28 eV and have a Gaussian distribution with 0.18 eV semidispersion. These results indicate that the rate limiting step in the effusion is the breaking of deuterium chemical bonds with the BN atomic network.

When deuteration occurs by D_2 ion implantation, the effusion process from h-BN thin films is controlled by the thermally activated diffusion of deuterium atoms to the sample surface: the measured diffusion constant exhibits an activation energy of 0.52 ± 0.03 eV and a pre-exponential factor in the 10^{-9} cm^2 s^{-1} order, indicating that migration occurs through grain boundaries of the nanostructured thin films.

Secondary ions mass spectroscopy (SIMS) measurements would be very useful to provide the distribution profiles of absorbed or implanted deuterium prior to the TDS procedures, as well as ERDA analysis: we plan to perform such analysis in a future work.

Acknowledgments

We are very grateful to R Tonini, Dipartimento di Fisica dell'Università di Modena, for deuterium ion implantation.

References

[1] Hirayama M and Shonho K 1980 *J. Electrochem. Soc.* **127** 399
[2] Friedmann T A *et al* 1994 *J. Appl. Phys.* **76** 3088
[3] Yoshida T 1996 *Diamond Relat. Mater.* **5** 501
[4] Widany J, Sternberg M and Frauenheim T 1997 *Solid State Commun.* **102** 451
[5] Kuhr M, Freudenstein R, Reinke S, Kuhlisch W, Dollinger G and Bergmaier A 1995 *J. Chem. Vapor Deposition* **3** 259
[6] Checchetto R, Chayahara A, Horino H, Miotello A and Fujii K 1997 *Thin Solid Films* **299** 5
[7] Bonizzi A, Checchetto R, Miotello A and Ossi P 1998 *Europhys. Lett.* **44** 627
[8] Ziegler J F, Biersack J P and Littman U 1985 *The Stopping and Range of Ions in Solids* (New York: Pergamon)
[9] Checchetto R, Gratton L M, Miotello A and Cestari C 1995 *Meas. Sci. Technol.* **6** 1605
[10] Dupasquier A and Mills A P Jr (eds) 1995 *Positron Spectroscopy of Solids* (Amsterdam: North-Holland)
[11] Cerofolini G F and Re N 1995 *J. Colloid Interface Sci.* **174** 428
[12] Koehler B G, Mak C H, Arthur D A, Coon P A and George S M 1988 *J. Chem. Phys.* **89** 1709
[13] Weast R C (ed) 1997 *CRC Handbook of Chemistry and Physics* (West Palm Beach, FL: Chemical Rubber Company)
[14] Elshabini-Riad A and Barlow F D III (eds) 1998 *Thin Film Technology Handbook (Electronic Packaging and Interconnection Series)* (New York: McGraw-Hill)
[15] Akkerman Z L, Kosinova M L, Fer N I, Rumjantsev Y M and Sysoeva N P 1990 *Thin Solid Films* **260** 156
[16] Rinnert H, Vergnat M, Marchal G and Burneau A 1997 *Appl. Surf. Sci.* **119** 224
[17] Checchetto R, Gratton L M, Miotello A, Tomasi A and Scardi P 1998 *Phys. Rev.* B **58** 4130
[18] Park J H, Choi J B, Kim H Y, Lee K J and Lee J Y 1995 *Thin Solid Films* **266** 129
[19] Acco S, Beyer W, van Fassen E E and van der Weg W F 1997 *J. Appl. Phys.* **82** 2862
[20] Checchetto R and Miotello A 2000 *J. Appl. Phys.* **87** 110
[21] Shewmon P 1989 *Diffusion in Solids* (Warrendale, PA: Minerals, Metal and Material Society)
[22] Brusa R S, Duarte Naia M, Zecca A, Nobili C, Ottavini G, Tonini R and Dupasquier A 1994 *Phys. Rev.* B **49** 7271
[23] Brusa R S, Karwasz G P, Tiengo N, Zecca A, Corni F, Ottavini G and Tonini R 2000 *Phys. Rev.* B **61** 10 154
[24] Cerofolini G C, Corni F, Fabbroni S, Nobili C, Ottaviani G and Tonini R 2000 *Mater. Sci. Eng.* **237** 1
[25] Lusson L, Elkaim P, Correia A and Ballutaud D 1995 *J. Physique* III **5** 1173
[26] Andrew P L and Haasz AA 1992 *J. Appl. Phys.* **72** 2749